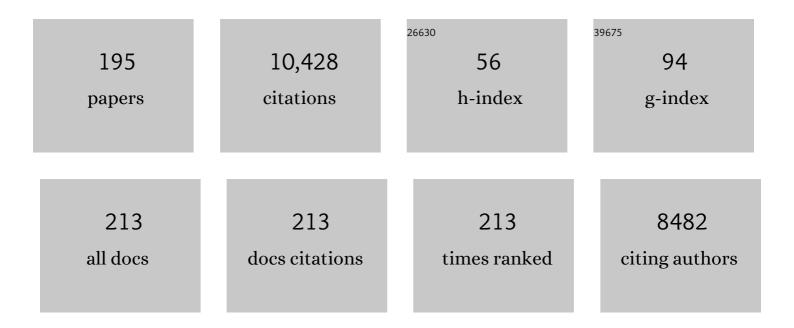
Julie V Macpherson

List of Publications by Year in descending order

Source: https://exaly.com/author-pdf/4430645/publications.pdf Version: 2024-02-01



LILLE V MACDHEDSON

#	Article	IF	CITATIONS
1	A practical guide to using boron doped diamond in electrochemical research. Physical Chemistry Chemical Physics, 2015, 17, 2935-2949.	2.8	426
2	Combined Scanning Electrochemicalâ ^{~,} Atomic Force Microscopy. Analytical Chemistry, 2000, 72, 276-285.	6.5	365
3	Conductive diamond: synthesis, properties, and electrochemical applications. Chemical Society Reviews, 2019, 48, 157-204.	38.1	333
4	Electrochemistry at carbon nanotubes: perspective and issues. Chemical Communications, 2009, , 6886.	4.1	285
5	Electrochemical Templating of Metal Nanoparticles and Nanowires on Single-Walled Carbon Nanotube Networks. Journal of the American Chemical Society, 2005, 127, 10639-10647.	13.7	241
6	A New View of Electrochemistry at Highly Oriented Pyrolytic Graphite. Journal of the American Chemical Society, 2012, 134, 20117-20130.	13.7	228
7	Carbon nanotube tips for atomic force microscopy. Nature Nanotechnology, 2009, 4, 483-491.	31.5	222
8	Topographical and electrochemical nanoscale imaging of living cells using voltage-switching mode scanning electrochemical microscopy. Proceedings of the National Academy of Sciences of the United States of America, 2012, 109, 11540-11545.	7.1	198
9	Fabrication and characterisation of nanometre-sized platinum electrodes for voltammetric analysis and imaging. Electrochemistry Communications, 1999, 1, 282-288.	4.7	187
10	Scanning Micropipet Contact Method for High-Resolution Imaging of Electrode Surface Redox Activity. Analytical Chemistry, 2009, 81, 2486-2495.	6.5	184
11	Examination of the Factors Affecting the Electrochemical Performance of Oxygen-Terminated Polycrystalline Boron-Doped Diamond Electrodes. Analytical Chemistry, 2013, 85, 7230-7240.	6.5	169
12	Structural Correlations in Heterogeneous Electron Transfer at Monolayer and Multilayer Graphene Electrodes. Journal of the American Chemical Society, 2012, 134, 7258-7261.	13.7	157
13	Boron Doped Diamond: A Designer Electrode Material for the Twenty-First Century. Annual Review of Analytical Chemistry, 2018, 11, 463-484.	5.4	152
14	Scanning Electrochemical Microscopy (SECM) as a Probe of Transfer Processes in Two-Phase Systems: Theory and Experimental Applications of SECM-Induced Transfer with Arbitrary Partition Coefficients, Diffusion Coefficients, and Interfacial Kinetics. Journal of Physical Chemistry B, 1998, 102, 1586-1598.	2.6	151
15	In-Situ Imaging of Ionic Crystal Dissolution Using an Integrated Electrochemical/AFM Probe. Journal of the American Chemical Society, 1996, 118, 6445-6452.	13.7	148
16	Factors Controlling the Electrodeposition of Metal Nanoparticles on Pristine Single Walled Carbon Nanotubes. Nano Letters, 2007, 7, 51-57.	9.1	147
17	Noncontact Electrochemical Imaging with Combined Scanning Electrochemical Atomic Force Microscopy. Analytical Chemistry, 2001, 73, 550-557.	6.5	145
18	Visualizing Zeptomole (Electro)Catalysis at Single Nanoparticles within an Ensemble. Journal of the American Chemical Society, 2011, 133, 10744-10747.	13.7	144

#	Article	IF	CITATIONS
19	Scanning electrochemical microscopy: beyond the solid/liquid interface. Analytica Chimica Acta, 1999, 385, 223-240.	5.4	143
20	Comparison and Reappraisal of Carbon Electrodes for the Voltammetric Detection of Dopamine. Analytical Chemistry, 2013, 85, 11755-11764.	6.5	143
21	Impact of Grain-Dependent Boron Uptake on the Electrochemical and Electrical Properties of Polycrystalline Boron Doped Diamond Electrodes. Journal of Physical Chemistry B, 2006, 110, 5639-5646.	2.6	137
22	Electrodeposition of Nickel Hydroxide Nanoparticles on Boron-Doped Diamond Electrodes for Oxidative Electrocatalysis. Journal of Physical Chemistry C, 2011, 115, 1649-1658.	3.1	134
23	Addressing the practicalities of anodic stripping voltammetry for heavy metal detection: a tutorial review. Analyst, The, 2019, 144, 6834-6849.	3.5	132
24	Nanowire Probes for High Resolution Combined Scanning Electrochemical Microscopy â^' Atomic Force Microscopy. Nano Letters, 2005, 5, 639-643.	9.1	125
25	Amperometric Oxygen Sensor Based on a Platinum Nanoparticle-Modified Polycrystalline Boron Doped Diamond Disk Electrode. Analytical Chemistry, 2009, 81, 1023-1032.	6.5	115
26	Scanning electrochemical microscopy: principles and applications to biophysical systems. Physiological Measurement, 2006, 27, R63-R108.	2.1	112
27	Electrochemical Mapping Reveals Direct Correlation between Heterogeneous Electronâ€Transfer Kinetics and Local Density of States in Diamond Electrodes. Angewandte Chemie - International Edition, 2012, 51, 7002-7006.	13.8	104
28	Ultrasensitive Detection of Dopamine Using a Carbon Nanotube Network Microfluidic Flow Electrode. Analytical Chemistry, 2013, 85, 163-169.	6.5	102
29	Single-Walled Carbon Nanotube Networks Decorated with Silver Nanoparticles:  A Novel Graded SERS Substrate. Journal of Physical Chemistry C, 2007, 111, 16167-16173.	3.1	100
30	Synthesis of azide/alkyne-terminal polymers and application for surface functionalisation through a [2 + 3] Huisgen cycloaddition process, "click chemistry― Soft Matter, 2007, 3, 732-739.	2.7	96
31	Electrochemical Imaging of Diffusion through Single Nanoscale Pores. Analytical Chemistry, 2002, 74, 1841-1848.	6.5	93
32	Quantitative nanoscale visualization of heterogeneous electron transfer rates in 2D carbon nanotube networks. Proceedings of the National Academy of Sciences of the United States of America, 2012, 109, 11487-11492.	7.1	93
33	Microjet Electrode: A Hydrodynamic Ultramicroelectrode with High Mass-Transfer Rates. Analytical Chemistry, 1994, 66, 2175-2179.	6.5	88
34	Determination of the Diffusion Coefficient of Hydrogen in Aqueous Solution Using Single and Double Potential Step Chronoamperometry at a Disk Ultramicroelectrode. Analytical Chemistry, 1997, 69, 2063-2069.	6.5	85
35	A Novel Approach to the Study of Dissolution Kinetics Using the Scanning Electrochemical Microscope: Theory and Application to Copper Sulfate Pentahydrate Dissolution in Aqueous Sulfuric Acid Solutions. The Journal of Physical Chemistry, 1994, 98, 1704-1713.	2.9	84
36	Mapping Nanoscale Electrochemistry of Individual Single-Walled Carbon Nanotubes. Nano Letters, 2014, 14, 220-224.	9.1	83

#	Article	IF	CITATIONS
37	Trace voltammetric detection of serotonin at carbon electrodes: comparison of glassy carbon, boron doped diamond and carbon nanotube network electrodes. Physical Chemistry Chemical Physics, 2010, 12, 10108.	2.8	81
38	Peer Reviewed: Atomic Force Microscopy Probes Go Electrochemical. Analytical Chemistry, 2002, 74, 576 A-584 A.	6.5	80
39	Electrochemical X-ray Fluorescence Spectroscopy for Trace Heavy Metal Analysis: Enhancing X-ray Fluorescence Detection Capabilities by Four Orders of Magnitude. Analytical Chemistry, 2014, 86, 4566-4572.	6.5	80
40	Trace Level Cyclic Voltammetry Facilitated by Single-Walled Carbon Nanotube Network Electrodes. Journal of the American Chemical Society, 2007, 129, 10982-10983.	13.7	79
41	Examination of the Spatially Heterogeneous Electroactivity of Boron-Doped Diamond Microarray Electrodes. Analytical Chemistry, 2006, 78, 2539-2548.	6.5	77
42	Electrochemical Nucleation and Growth of Gold Nanoparticles on Single-Walled Carbon Nanotubes: New Mechanistic Insights. Journal of Physical Chemistry C, 2010, 114, 13241-13248.	3.1	77
43	Fabrication of Versatile Channel Flow Cells for Quantitative Electroanalysis Using Prototyping. Analytical Chemistry, 2010, 82, 3124-3131.	6.5	77
44	Scanning Electrochemical Microscopy as a Local Probe of Oxygen Permeability in Cartilage. Biophysical Journal, 2000, 78, 1578-1588.	0.5	74
45	Characterization of Batch-Microfabricated Scanning Electrochemical-Atomic Force Microscopy Probes. Analytical Chemistry, 2005, 77, 424-434.	6.5	74
46	Tracking Metal Electrodeposition Dynamics from Nucleation and Growth of a Single Atom to a Crystalline Nanoparticle. ACS Nano, 2018, 12, 7388-7396.	14.6	74
47	Measurement of Local Reactivity at Liquid/Solid, Liquid/Liquid, and Liquid/Gas Interfaces with the Scanning Electrochemical Microscope:  Principles, Theory, and Applications of the Double Potential Step Chronoamperometric Mode. Journal of Physical Chemistry B, 1997, 101, 10851-10859.	2.6	73
48	Active Sites for Outer-Sphere, Inner-Sphere, and Complex Multistage Electrochemical Reactions at Polycrystalline Boron-Doped Diamond Electrodes (pBDD) Revealed with Scanning Electrochemical Cell Microscopy (SECCM). Analytical Chemistry, 2012, 84, 5427-5432.	6.5	73
49	Functionalizing Single-Walled Carbon Nanotube Networks:  Effect on Electrical and Electrochemical Properties. Journal of Physical Chemistry C, 2007, 111, 12944-12953.	3.1	69
50	Factors Controlling Stripping Voltammetry of Lead at Polycrystalline Boron Doped Diamond Electrodes: New Insights from High-Resolution Microscopy. Analytical Chemistry, 2011, 83, 735-745.	6.5	68
51	Characterisation and behaviour of Ti/TiO2/noble metal anodes. Electrochimica Acta, 2003, 48, 1131-1141.	5.2	64
52	<i>In Situ</i> Optimization of pH for Parts-Per-Billion Electrochemical Detection of Dissolved Hydrogen Sulfide Using Boron Doped Diamond Flow Electrodes. Analytical Chemistry, 2014, 86, 10834-10840.	6.5	63
53	Scanning Electrochemical Microscope Induced Dissolution: Rate Law and Reaction Rate Imaging for Dissolution of the (010) Face of Potassium Ferrocyanide Trihydrate in Nonstoichiometric Aqueous Solutions of the Lattice Ions. The Journal of Physical Chemistry, 1995, 99, 3338-3351.	2.9	62
54	Imaging local mass-transfer rates within an impinging jet and studies of fast heterogeneous electron-transfer kinetics using the microjet electrode. Journal of the Chemical Society, Faraday Transactions, 1995, 91, 899.	1.7	62

#	Article	IF	CITATIONS
55	Nanoscale Imaging of the Electronic Conductivity of the Native Oxide Film on Titanium Using Conducting Atomic Force Microscopy. Journal of Physical Chemistry B, 2003, 107, 9677-9680.	2.6	58
56	Electrochemistry at Nanoscale Electrodes: Individual Single-Walled Carbon Nanotubes (SWNTs) and SWNT-Templated Metal Nanowires. ACS Nano, 2011, 5, 10017-10025.	14.6	58
57	Electron Transfer Kinetics at Single-Walled Carbon Nanotube Electrodes using Scanning Electrochemical Microscopy. Journal of Physical Chemistry C, 2010, 114, 2633-2639.	3.1	57
58	Radial Flow Microring Electrode:Â Investigation of Fast Heterogeneous Electron-Transfer Processes. Journal of Physical Chemistry B, 1998, 102, 9891-9897.	2.6	55
59	Single-Walled Carbon Nanotube Network Ultramicroelectrodes. Analytical Chemistry, 2008, 80, 3598-3605.	6.5	55
60	New strategies for probing crystal dissolution kinetics at the microscopic level. Chemical Society Reviews, 1995, 24, 109.	38.1	53
61	Observation and characterisation of the glycocalyx of viable human endothelial cells using confocal laser scanning microscopy. Physical Chemistry Chemical Physics, 2004, 6, 1006-1011.	2.8	53
62	An unusual soluble β-turn-rich conformation of prion is involved in fibril formation and toxic to neuronal cells. Biochemical and Biophysical Research Communications, 2005, 328, 292-305.	2.1	53
63	Ultrathin Carbon Nanotube Mat Electrodes for Enhanced Amperometric Detection. Advanced Materials, 2009, 21, 3105-3109.	21.0	53
64	Formation of polyaniline/Pt nanoparticle composite films and their electrocatalytic properties. Journal of Solid State Electrochemistry, 2006, 10, 792-807.	2.5	52
65	Electrochemical Flow Injection Analysis of Hydrazine in an Excess of an Active Pharmaceutical Ingredient: Achieving Pharmaceutical Detection Limits Electrochemically. Analytical Chemistry, 2015, 87, 10064-10071.	6.5	52
66	Scanning Electrochemical Microscope-Induced Dissolution:Â Theory and Experiment for Silver Chloride Dissolution Kinetics in Aqueous Solution without Supporting Electrolyte. The Journal of Physical Chemistry, 1996, 100, 19475-19483.	2.9	51
67	Boron doped diamond ultramicroelectrodes: a generic platform for sensing single nanoparticle electrocatalytic collisions. Chemical Communications, 2013, 49, 5657.	4.1	50
68	Electrodeposition of Nickel Hydroxide Nanoparticles on Carbon Nanotube Electrodes: Correlation of Particle Crystallography with Electrocatalytic Properties. Journal of Physical Chemistry C, 2016, 120, 16059-16068.	3.1	50
69	Controlled sp ² Functionalization of Boron Doped Diamond as a Route for the Fabrication of Robust and Nernstian pH Electrodes. Analytical Chemistry, 2016, 88, 974-980.	6.5	49
70	Single-Wall Carbon Nanotube Conducting Probe Tips. Journal of Physical Chemistry B, 2002, 106, 13102-13105.	2.6	48
71	Imaging the Action of Fluid Flow Blocking Agents on Dentinal Surfaces Using a Scanning Electrochemical Microscope. Langmuir, 1995, 11, 3959-3963.	3.5	47
72	Probing the oxidative etching kinetics of metals with the feedback mode of the scanning electrochemical microscope. Journal of the Chemical Society, Faraday Transactions, 1996, 92, 3799.	1.7	47

#	Article	IF	CITATIONS
73	On the microelectrode behaviour of graphite–epoxy composite electrodes. Electrochemistry Communications, 2002, 4, 245-250.	4.7	47
74	Controlled Growth and Characterization of Two-Dimensional Single-Walled Carbon-Nanotube Networks for Electrical Applications. Small, 2007, 3, 860-870.	10.0	46
75	Electrochemical and Conductivity Measurements of Single-Wall Carbon Nanotube Network Electrodes. Journal of the American Chemical Society, 2004, 126, 16724-16725.	13.7	45
76	In Situ Observation of the Surface Processes Involved in Dissolution from the Cleavage Surface of Calcite in Aqueous Solution Using Combined Scanning Electrochemical-Atomic Force Microscopy (SECM-AFM). ChemPhysChem, 2003, 4, 139-146.	2.1	44
77	Lifting the lid on the potentiostat: a beginner's guide to understanding electrochemical circuitry and practical operation. Physical Chemistry Chemical Physics, 2021, 23, 8100-8117.	2.8	44
78	Molecular Ordering and 2D Conductivity in Ultrathin Poly(3-hexylthiophene)/Gold Nanoparticle Composite Films. Journal of Physical Chemistry B, 2005, 109, 19335-19344.	2.6	42
79	Hydrodynamic ultramicroelectrodes: kinetic and analytical applications. Electrochimica Acta, 2001, 47, 29-45.	5.2	41
80	Correlation of membrane structure and transport activity using combined scanning electrochemical–atomic force microscopy. Electrochemistry Communications, 2005, 7, 612-618.	4.7	41
81	Investigation of film formation properties during electrochemical oxidation of serotonin (5-HT) at polycrystalline boron doped diamond. Physical Chemistry Chemical Physics, 2013, 15, 18085.	2.8	41
82	Scanning electrochemical microscopy as a probe of local fluid flow through porous solids. Journal of the Chemical Society, Faraday Transactions, 1995, 91, 1407.	1.7	40
83	Radial Flow Microring Electrode:  Development and Characterization. Analytical Chemistry, 1998, 70, 2914-2921.	6.5	40
84	Evanescent Wave Cavity Ring-Down Spectroscopy in a Thin-Layer Electrochemical Cell. Analytical Chemistry, 2006, 78, 6833-6839.	6.5	39
85	Impact of Adsorption on Scanning Electrochemical Microscopy Voltammetry and Implications for Nanogap Measurements. Analytical Chemistry, 2016, 88, 3272-3280.	6.5	39
86	Deconvoluting Surface-Bound Quinone Proton Coupled Electron Transfer in Unbuffered Solutions: Toward a Universal Voltammetric pH Electrode. Journal of the American Chemical Society, 2019, 141, 1035-1044.	13.7	38
87	High-Resolution Electrochemical, Electrical, and Structural Characterization of a Dimensionally Stable Ti/TiO[sub 2]/Pt Electrode. Journal of the Electrochemical Society, 2002, 149, B306.	2.9	37
88	In Situ Control of Local pH Using a Boron Doped Diamond Ring Disk Electrode: Optimizing Heavy Metal (Mercury) Detection. Analytical Chemistry, 2014, 86, 367-371.	6.5	37
89	Horizontal Alignment of Chemical Vapor-Deposited SWNTs on Single-Crystal Quartz Surfaces: Further Evidence for Epitaxial Alignment. Journal of Physical Chemistry C, 2009, 113, 17087-17096.	3.1	36
90	Direct Identification and Analysis of Heavy Metals in Solution (Hg, Cu, Pb, Zn, Ni) by Use of in Situ Electrochemical X-ray Fluorescence. Analytical Chemistry, 2015, 87, 4933-4940.	6.5	36

#	Article	IF	CITATIONS
91	Effect of composition on the conductivity and morphology of poly(3-hexylthiophene)/gold nanoparticle composite Langmuir–Schaeffer films. Physical Chemistry Chemical Physics, 2006, 8, 5096-5105.	2.8	34
92	<i>In situ</i> scanning electrochemical probe microscopy for energy applications. MRS Bulletin, 2012, 37, 668-674.	3.5	34
93	Electrochemical Synthesis of Nanoporous Platinum Nanoparticles Using Laser Pulse Heating: Application to Methanol Oxidation. ACS Catalysis, 2017, 7, 7388-7398.	11.2	34
94	Single-Walled Carbon Nanotubes as Templates for Nanowire Conducting Probes. Nano Letters, 2003, 3, 1365-1369.	9.1	33
95	Electro-oxidation of hydrazine at gold nanoparticle functionalised single walled carbon nanotube network ultramicroelectrodes. Physical Chemistry Chemical Physics, 2011, 13, 17146.	2.8	33
96	Nanoscale Reactivity Mapping of a Single-Crystal Boron-Doped Diamond Particle. Analytical Chemistry, 2021, 93, 5831-5838.	6.5	33
97	Combined scanning electrochemical-atomic force microscopy (SECM-AFM): Simulation and experiment for flux-generation at un-insulated metal-coated probes. Journal of Electroanalytical Chemistry, 2005, 585, 8-18.	3.8	32
98	Effects of Metal Underlayer Grain Size on Carbon Nanotube Growth. Journal of Physical Chemistry C, 2009, 113, 15133-15139.	3.1	32
99	Assessment of acid and thermal oxidation treatments for removing sp2 bonded carbon from the surface of boron doped diamond. Carbon, 2020, 167, 1-10.	10.3	32
100	In Situ Observation of the Surface Processes Involved in Dissolution from the (010) Surface of Potassium Ferrocyanide Trihydrate in Aqueous Solution Using an Integrated Electrochemicalâ^'Atomic Force Microscope. Journal of Physical Chemistry B, 2000, 104, 2351-2359.	2.6	31
101	Assessment of the Electrochemical Behavior of Two-Dimensional Networks of Single-Walled Carbon Nanotubes. Analytical Chemistry, 2006, 78, 7006-7015.	6.5	31
102	In-Situ Atomic Force Microscopy (AFM) Imaging: Influence of AFM Probe Geometry on Diffusion to Microscopic Surfaces. Langmuir, 2008, 24, 12867-12876.	3.5	30
103	Enhancing Square Wave Voltammetry Measurements via Electrochemical Analysis of the Non-Faradaic Potential Window. Analytical Chemistry, 2019, 91, 7935-7942.	6.5	30
104	An sp ² Patterned Boron Doped Diamond Electrode for the Simultaneous Detection of Dissolved Oxygen and pH. ACS Sensors, 2019, 4, 756-763.	7.8	30
105	Electrochemical impedance spectroscopy at single-walled carbon nanotube network ultramicroelectrodes. Electrochemistry Communications, 2009, 11, 2081-2084.	4.7	29
106	Electron beam lithographically-defined scanning electrochemical-atomic force microscopy probes: fabrication method and application to high resolution imaging on heterogeneously active surfaces. Physical Chemistry Chemical Physics, 2006, 8, 3909.	2.8	27
107	Effect of high rates of mass transport on oxygen reduction at copper electrodes: Implications for aluminium corrosion. Electrochemistry Communications, 2008, 10, 1334-1336.	4.7	27
108	Fabrication Route for the Production of Coplanar, Diamond Insulated, Boron Doped Diamond Macro- and Microelectrodes of any Geometry. Analytical Chemistry, 2014, 86, 5238-5244.	6.5	27

#	Article	IF	CITATIONS
109	Quinone electrochemistry for the comparative assessment of sp 2 surface content of boron doped diamond electrodes. Electrochemistry Communications, 2016, 72, 59-63.	4.7	27
110	Boron Doped Diamond as a Low Biofouling Material in Aquatic Environments: Assessment of <i>Pseudomonas aeruginosa</i> Biofilm Formation. ACS Applied Materials & Interfaces, 2019, 11, 25024-25033.	8.0	27
111	Local amperometric detection of K+ in aqueous solution using scanning electrochemical microscopy ion-transfer voltammetry. Electrochemistry Communications, 2000, 2, 201-206.	4.7	26
112	Atomic Force Microscopy Investigation of the Mechanism of Calcite Microcrystal Growth under Kitano Conditions. Langmuir, 2005, 21, 1255-1260.	3.5	25
113	Evanescent Wave Cavity Ring-Down Spectroscopy as a Probe of Interfacial Adsorption: Interaction of Tris(2,2′-bipyridine)ruthenium(II) with Silica Surfaces and Polyelectrolyte Films. Langmuir, 2009, 25, 248-255.	3.5	25
114	Hydrodynamic Modulation Voltammetry with an Oscillating Microjet Electrode. Analytical Chemistry, 1999, 71, 4642-4648.	6.5	24
115	Influence of ultrathin poly-(3,4-ethylenedioxythiophene) (PEDOT) film supports on the electrodeposition and electrocatalytic activity of discrete platinum nanoparticles. Journal of Solid State Electrochemistry, 2011, 15, 2331-2339.	2.5	24
116	Comparison of fast electron transfer kinetics at platinum, gold, glassy carbon and diamond electrodes using Fourier-transformed AC voltammetry and scanning electrochemical microscopy. Physical Chemistry Chemical Physics, 2017, 19, 8726-8734.	2.8	24
117	High pressure high temperature synthesis of highly boron doped diamond microparticles and porous electrodes for electrochemical applications. Carbon, 2021, 171, 845-856.	10.3	24
118	Surface Assembly and Redox Dissolution of Silver Nanoparticles Monitored by Evanescent Wave Cavity Ring-Down Spectroscopy. Journal of Physical Chemistry C, 2008, 112, 15274-15280.	3.1	23
119	Pt nanoparticle modified single walled carbon nanotube network electrodes for electrocatalysis: Control of the specific surface area over three orders of magnitude. Catalysis Today, 2015, 244, 136-145.	4.4	22
120	Facetâ€Resolved Electrochemistry of Polycrystalline Boronâ€Doped Diamond Electrodes: Microscopic Factors Determining the Solvent Window in Aqueous Potassium Chloride Solutions. ChemElectroChem, 2018, 5, 3028-3035.	3.4	22
121	Hydrodynamics and Mass Transport in Wall Tube and Microjet Electrodes. Simulation and Experiment for Micrometer-Scale Electrodes. Journal of Physical Chemistry B, 2003, 107, 379-386.	2.6	22
122	Silverâ€decorated carbon nanotube networks as SERS substrates. Journal of Raman Spectroscopy, 2011, 42, 1255-1262.	2.5	21
123	Diminished Electron Transfer Kinetics for [Ru(NH ₃) ₆] ^{3+/2+} , [α-SiW ₁₂ O ₄₀] ^{4–/5–} , and [α-SiW ₁₂ O ₄₀] ^{5–/6–} Processes at Boron-Doped Diamond Electrodes. Iournal of Physical Chemistry C. 2015. 119. 12464-12472.	3.1	21
124	Impact of chemical vapour deposition plasma inhomogeneity on the spatial variation of sp2 carbon in boron doped diamond electrodes. Carbon, 2017, 121, 434-442.	10.3	21
125	Faraday communications. A new approach to the study of dissolution kinetics. Journal of the Chemical Society, Faraday Transactions, 1993, 89, 1883.	1.7	20
126	Single walled carbon nanotube channel flow electrode: Hydrodynamic voltammetry at the nanomolar level. Electrochemistry Communications, 2011, 13, 186-189.	4.7	20

#	Article	IF	CITATIONS
127	Hydrodynamic Modulation Voltammetry with a Variable-Height Radial Flow Microring Electrode. Analytical Chemistry, 1999, 71, 2939-2944.	6.5	19
128	Recent Advances in Hydrodynamic Modulation Voltammetry. Electroanalysis, 2000, 12, 1001-1011.	2.9	19
129	Conducting-Atomic Force Microscopy Investigation of the Local Electrical Characteristics of a Ti/TiO[sub 2]/Pt Anode. Electrochemical and Solid-State Letters, 2001, 4, E33.	2.2	19
130	Enhanced resolution electric force microscopy with single-wall carbon nanotube tips. Journal of Applied Physics, 2004, 96, 3565-3567.	2.5	19
131	Impact of sp ² Carbon Edge Effects on the Electron-Transfer Kinetics of the Ferrocene/Ferricenium Process at a Boron-Doped Diamond Electrode in an Ionic Liquid. Journal of Physical Chemistry C, 2019, 123, 17397-17406.	3.1	19
132	Selection, characterisation and mapping of complex electrochemical processes at individual single-walled carbon nanotubes: the case of serotonin oxidation. Faraday Discussions, 2014, 172, 439-455.	3.2	17
133	Electrochemical electron paramagnetic resonance utilizing loop gap resonators and micro-electrochemical cells. Physical Chemistry Chemical Physics, 2015, 17, 23438-23447.	2.8	17
134	Controlled functionalisation of single-walled carbon nanotube network electrodes for the enhanced voltammetric detection of dopamine. Physical Chemistry Chemical Physics, 2015, 17, 26394-26402.	2.8	17
135	Electrochemical "read–write―microscale patterning of boron doped diamond electrodes. Chemical Communications, 2015, 51, 164-167.	4.1	17
136	Scanning electrochemical microscopy as a probe of Ag+ binding kinetics at Langmuir phospholipid monolayers. Physical Chemistry Chemical Physics, 2005, 7, 2955.	2.8	16
137	Characterization and Application of a Mercury Hemisphere Microjet Electrode. Analytical Chemistry, 1997, 69, 5045-5051.	6.5	15
138	Production and Properties of Nanoelectrospray Emitters Used in Fourier Transform Ion Cyclotron Resonance Mass Spectrometry:Â Implications for Determination of Association Constants for Noncovalent Complexes. Analytical Chemistry, 2004, 76, 5172-5179.	6.5	14
139	Fabrication and Characterization of an All-Diamond Tubular Flow Microelectrode for Electroanalysis. Analytical Chemistry, 2011, 83, 5804-5808.	6.5	14
140	Intrinsic electrochemical activity of single walled carbon nanotube–Nafion assemblies. Physical Chemistry Chemical Physics, 2013, 15, 5030.	2.8	14
141	Elucidating the Cathodic Electrodeposition Mechanism of Lead/Lead Oxide Formation in Nitrate Solutions. Journal of Physical Chemistry C, 2017, 121, 6835-6843.	3.1	14
142	Exploring the suitability of different electrode materials for hypochlorite quantification at high concentration in alkaline solutions. Electrochemistry Communications, 2018, 86, 21-25.	4.7	14
143	Laser heated boron doped diamond electrodes: effect of temperature on outer sphere electron transfer processes. Faraday Discussions, 2014, 172, 421-438.	3.2	13
144	Intermittentâ€contact Scanning Electrochemical Microscopy (ICâ€SECM) as a Quantitative Probe of Defects in Single Crystal Boron Doped Diamond Electrodes. Electroanalysis, 2016, 28, 2297-2302.	2.9	13

#	Article	IF	CITATIONS
145	Electrochemistry of single nanoparticles: general discussion. Faraday Discussions, 2016, 193, 387-413.	3.2	13
146	Probing Electrode Heterogeneity Using Fourier-Transformed Alternating Current Voltammetry: Application to a Dual-Electrode Configuration. Analytical Chemistry, 2017, 89, 2830-2837.	6.5	13
147	Investigation of sp ² -Carbon Pattern Geometry in Boron-Doped Diamond Electrodes for the Electrochemical Quantification of Hypochlorite at High Concentrations. ACS Sensors, 2020, 5, 789-797.	7.8	13
148	Manipulation and measurement of pH sensitive metal–ligand binding using electrochemical proton generation and metal detection. Chemical Communications, 2016, 52, 1863-1866.	4.1	12
149	<i>Ex Vivo</i> Electrochemical pH Mapping of the Gastrointestinal Tract in the Absence and Presence of Pharmacological Agents. ACS Sensors, 2020, 5, 2858-2865.	7.8	12
150	Visualisation of electrochemical processes at optically transparent carbon nanotube ultramicroelectrodes (OT-CNT-UMEs). Physical Chemistry Chemical Physics, 2011, 13, 5223.	2.8	11
151	Selective Detection of Hydrazine in the Presence of Excess Electrochemically Active Pharmaceutical Ingredients Using Boron Doped Diamond Metal Nanoparticle Functionalised Electrodes. Electroanalysis, 2013, 25, 2613-2619.	2.9	11
152	Carbon electrodes for energy storage: general discussion. Faraday Discussions, 2014, 172, 239-260.	3.2	11
153	Quantitative analysis of trace palladium contamination in solution using electrochemical X-ray fluorescence (EC-XRF). Analyst, The, 2016, 141, 3349-3357.	3.5	10
154	Miniaturized probe on polymer SU-8 with array of individually addressable microelectrodes for electrochemical analysis in neural and other biological tissues. Analytical and Bioanalytical Chemistry, 2021, 413, 6777-6791.	3.7	10
155	Coexistence of carbonyl and ether groups on oxygen-terminated (110)-oriented diamond surfaces. Communications Materials, 2022, 3, .	6.9	10
156	Laser Scanning Confocal Microscopy Coupled with Hydraulic Permeability Measurements for Elucidating Fluid Flow across Porous Materials: Application to Human Dentine. Analytical Sciences, 2008, 24, 437-442.	1.6	9
157	Pulling Nanotubes from Supported Bilayers. Langmuir, 2011, 27, 8269-8274.	3.5	9
158	Electrochemical activation of pristine single walled carbon nanotubes: impact on oxygen reduction and other surface sensitive redox processes. Physical Chemistry Chemical Physics, 2014, 16, 9966.	2.8	9
159	Fabrication of a single sub-micron pore spanning a single crystal (100) diamond membrane and impact on particle translocation. Carbon, 2017, 122, 319-328.	10.3	9
160	Influence of Tip and Substrate Properties and Nonsteady-State Effects on Nanogap Kinetic Measurements: Response to Comment on "Impact of Adsorption on Scanning Electrochemical Microscopy Voltammetry and Implications for Nanogap Measurementsâ€: Analytical Chemistry, 2017, 89, 7273-7276.	6.5	9
161	Switching on palladium catalyst electrochemical removal from a palladium acetate–acetonitrile system via trace water addition. Green Chemistry, 2019, 21, 4662-4672.	9.0	9
162	Controlling palladium morphology in electrodeposition from nanoparticles to dendrites <i>via</i> the use of mixed solvents. Nanoscale, 2020, 12, 21757-21769.	5.6	9

#	Article	IF	CITATIONS
163	Combined Voltammetric Measurement of pH and Free Chlorine Speciation Using a Micro-Spot sp ² Bonded Carbon–Boron Doped Diamond Electrode. Analytical Chemistry, 2020, 92, 16072-16078.	6.5	8
164	Ultrafast transient absorption spectroelectrochemistry: femtosecond to nanosecond excited-state relaxation dynamics of the individual components of an anthraquinone redox couple. Chemical Science, 2022, 13, 486-496.	7.4	8
165	Modes of Action of a Weak Acid Modifier of Calcite Growth. ChemPhysChem, 2006, 7, 1019-1021.	2.1	7
166	Field ionization using densely spaced arrays of nickel-tipped carbon nanotubes. Chemical Physics Letters, 2011, 505, 126-129.	2.6	7
167	Dual-electrode measurements in a meniscus microcapillary electrochemical cell using a high aspect ratio carbon fibre ultramicroelectrode. Journal of Electroanalytical Chemistry, 2014, 729, 80-86.	3.8	6
168	Quantitative measurements in electrochemical electron paramagnetic resonance. Electrochimica Acta, 2016, 213, 802-810.	5.2	6
169	Probing Electrode Heterogeneity using Fourier-Transformed Alternating Current Voltammetry: Protocol Development. Electrochimica Acta, 2017, 240, 514-521.	5.2	6
170	A synthetic diamond conductivity sensor: Design rules and applications. Sensors and Actuators B: Chemical, 2017, 238, 1128-1135.	7.8	6
171	Electrochemical Ozone Generation Using Compacted High Pressure High Temperature Synthesized Boron Doped Diamond Microparticle Electrodes. Journal of the Electrochemical Society, 2021, 168, 126514.	2.9	6
172	Probing Redox Reactions of Immobilized Cytochrome <i>c</i> Using Evanescent Wave Cavity Ringâ€Down Spectroscopy in a Thin‣ayer Electrochemical Cell. ChemPhysChem, 2010, 11, 2985-2991.	2.1	5
173	Versatile DIY Route for Incorporation of a Wide Range of Electrode Materials into Rotating Ring Disk Electrodes. Analytical Chemistry, 2022, 94, 9856-9862.	6.5	5
174	Taking a closer look at conductivity. Nature Nanotechnology, 2011, 6, 84-85.	31.5	4
175	The many faces of carbon in electrochemistry: general discussion. Faraday Discussions, 2014, 172, 117-137.	3.2	4
176	Atomic-scale investigation of the reversible α- to ï‰-phase lithium ion charge – discharge characteristics of electrodeposited vanadium pentoxide nanobelts. Journal of Materials Chemistry A, 2022, 10, 8515-8527.	10.3	4
177	Processes at nanopores and bio-nanointerfaces: general discussion. Faraday Discussions, 2018, 210, 145-171.	3.2	3
178	Formation of polyaniline/Pt nanoparticle composite films and their electrocatalytic properties. Journal of Solid State Electrochemistry, 2006, 10, 792-807.	2.5	3
179	Development of a Novel Combined Scanning Electrochemical Microscope (SECM) and Scanning Ion-Conductance Microscope (SICM) Probe for Soft Sample Imaging. Materials Research Society Symposia Proceedings, 2012, 1422, 13.	0.1	2
180	Assessment of Boron Doped Diamond Electrode Quality and Application to In Situ Modification of Local pH by Water Electrolysis. Journal of Visualized Experiments, 2016, , .	0.3	2

#	Article	IF	CITATIONS
181	Diamond membrane production: The critical role of radicals in the non-contact electrochemical etching of sp2 carbon. Carbon, 2021, 185, 717-726.	10.3	2

Innenrücktitelbild: Electrochemical Mapping Reveals Direct Correlation between Heterogeneous Electron-Transfer Kinetics and Local Density of States in Diamond ElectrodesZ203057 (Angew. Chem.) Tj ETQq0 0 @.gBT /Oværlock 10 T

183	Role of surface contaminants, functionalities, defects and electronic structure: general discussion. Faraday Discussions, 2014, 172, 365-395.	3.2	1
184	Investigation of molecular partitioning between non polar oil droplets and aqueous solution using double potential step chronoamperometry. Physical Chemistry Chemical Physics, 2014, 16, 10456-10463.	2.8	1
185	Carbon electrode interfaces for synthesis, sensing and electrocatalysis: general discussion. Faraday Discussions, 2014, 172, 497-520.	3.2	1
186	Nanopores: general discussion. Faraday Discussions, 2016, 193, 507-531.	3.2	1
187	Reactions at the nanoscale: general discussion. Faraday Discussions, 2016, 193, 265-292.	3.2	1
188	Processes at nanoelectrodes: general discussion. Faraday Discussions, 2018, 210, 235-265.	3.2	1
189	Identification of Mechanistic Subtleties that Apply to Voltammetric Studies at Boron-Doped Diamond Electrodes. Journal of Physical Chemistry C, 2020, 124, 24232-24244.	3.1	1
190	Atomic-Scale Investigation of the Reversible α- to ï‰-Phase Lithium Ion Charge – Discharge Characteristics of Electrodeposited Vanadium Pentoxide Nanobelts. ECS Meeting Abstracts, 2022, MA2022-01, 2129-2129.	0.0	1
191	Electron Beam Transparent Boron Doped Diamond Electrodes for Combined Electrochemistry─Transmission Electron Microscopy. ACS Measurement Science Au, 2022, 2, 439-448.	4.4	1
192	Themed issue on Bioelectrochemistry. Physical Chemistry Chemical Physics, 2010, 12, 9971.	2.8	0
193	Energy conversion at nanointerfaces: general discussion. Faraday Discussions, 2018, 210, 333-351.	3.2	0
194	Quantitative trace level voltammetry in the presence of electrode fouling agents: Comparison of single-walled carbon nanotube network electrodes and screen-printed carbon electrodes. Journal of Electroanalytical Chemistry, 2020, 872, 114137.	3.8	0
195	(Invited) Tracking Metal Electrodeposition Dynamics from Nucleation and Growth of a Single Atom to a Crystalline Nanoparticle. ECS Meeting Abstracts, 2022, MA2022-01, 1159-1159.	0.0	0